conduit networks fulfills a number of observational constraints including the rapid transport times required by recent U-Th disequilibrium (*11–13*) and ^{10}Be (*9*) studies, the observed episodicity of volcanic production at arcs (*1*), and ascent trajectories in *P-T* space that allow hydrous material to enter the subarc region within the melting field, avoiding substantial freezing out of melt during ascent. Rapid vertical transport along conduit networks may also explain the sustained, high-volume magmatism observed at some arcs (*23*).

References and Notes

1. B. D. Marsh, *J. Geol.* **87**, 687 (1979).
2. Y. Tamura, *J. Petrol.* **35**, 619 (1994).
3. M. Sakuyama, *J. Volcanol. Geotherm. Res.* **18**, 297 (1983).
4. Y. Tatsumi, M. Sakuyama, H. Fukuyama, I. Kushiro, *J. Geophys. Res.* **88**, 5815 (1983).
5. M. Nakada, Y. Takeda, *Tectonophysics* **246**, 147 (1995).
6. M. Spiegelman, D. McKenzie, *Earth Planet. Sci. Lett.* **83**, 137 (1987).
7. J. H. Davies, D. J. Stevenson, *J. Geophys. Res.* **97**, 2037 (1992).
8. Y. Furukawa, *J. Geophys. Res.* **98**, 8309 (1993).
9. J. D. Morris, W. P. Leeman, F. Tera, *Nature* **344**, 31 (1990).
10. M. T. McCulloch, J. A. Gamble, *Earth Planet. Sci. Lett.* **102**, 358 (1991).
11. C. J. Hawkesworth, S. P. Turner, F. McDermott, D. W. Peate, P. van Calsteren, *Science* **276**, 551 (1997).
12. S. Turner, C. Hawkesworth, *Nature* **389**, 568 (1997).
13. T. Elliott, T. Plank, A. Zindler, W. White, B. Bourdon, *J. Geophys. Res.* **102**, 14991 (1997).
14. P. R. Vogt, *Earth Planet. Sci. Lett.* **21**, 235 (1974).
15. R. D. Jarrard, *Rev. Geophys.* **24**, 217 (1986).
16. B. D. Marsh, I. S. E. Carmichael, *J. Geophys. Res.* **79**, 1196 (1974).
17. B. D. Marsh, *Am. Sci.* **67**, 161 (1979).
18. ———, in *The Geophysics of the Pacific Ocean Basin and Its Margins*, G. H. Sutton, M. H. Manghnani, R. Moberly, Eds. (American Geophysical Union, Washington, DC, 1976), vol. 19, pp. 337–350.
19. M. A. Feighner, L. H. Kellogg, B. J. Travis, *Geophys. Res. Lett.* **22**, 715 (1995).
20. P. Olson, H. Singer, *J. Fluid Mech.* **158**, 511 (1985).
21. J. A. Whitehead, K. R. Helfrich, in *Magma Transport and Storage*, M. P. Ryan, Ed. (Wiley, Chichester, UK, 1990), pp. 53–76.
22. B. D. Marsh, *Am. J. Sci.* **282**, 808 (1982).
23. J. Johnson, J. M. Lees, E. Gordeev, *Geophys. Res. Lett.* **25**, 3999 (1998).
24. D. H. Green, *Earth Planet. Sci. Lett.* **19**, 37 (1973).
25. A. B. Thompson, *Nature* **358**, 295 (1992).
26. D. McKenzie, M. J. Bickle, *J. Petrol.* **29**, 625 (1988).
27. C. Kincaid, I. S. Sacks, *J. Geophys. Res.* **102**, 12295 (1997).
28. G. Hirth, D. L. Kohlstedt, *Earth Planet. Sci. Lett.* **144**, 93 (1996).
29. ———, *J. Geophys. Res.* **100**, 15441 (1995).

30. This paper benefited from the input of the many participants at the August 2000 MARGINS Theoretical Institute in Eugene, OR, and two anonymous reviewers. This work was supported by NSF grants EAR-92-19796 and EAR-96-28739.

7 March 2001; accepted 25 May 2001

Evidence for a Large-Scale Remnant of Subducted Lithosphere Beneath Fiji

Wang-Ping Chen[1,2]* and Michael R. Brudzinski[1]

We combine spatial variations of *P*- and *S*-wave speeds, 1000 fault plane solutions, and 6600 well-determined hypocenters to investigate the nature of subducted lithosphere and deep earthquakes beneath the Tonga back-arc. We show that perplexing patterns in seismicity and fault plane solutions can be accounted for by the juxtaposition of a steep-dipping Wadati-Benioff zone and a subhorizontal remnant of slab that is no longer attached to the actively subducting lithosphere. The detached slab may be from a previous episode of subduction along the fossil Vitiaz trench about 5 to 8 million years ago. The juxtaposition of slabs retains a large amount of subducted material in the transition zone of the mantle. Such a configuration, if common in the past, would allow the preservation of a primordial component in the lower mantle.

The interaction between subducted lithosphere and the transition zone of the mantle is a key issue in geodynamics. In particular, the amount of slab penetration into the lower mantle controls the rate of heat and mass transfer between the upper and the lower mantle (*1–3*). The Tonga subduction zone is a natural laboratory for studying this issue because large amounts of old, cold slab have been rapidly subducting in the past 50 to 100 million years (*4–6*). Presently, the rate of subduction exceeds 200 ± 40 mm/year (*7*).

Considering the old age of the Pacific lithosphere being subducted and the extremely fast rate of convergence, subducted material beneath Tonga should have caused the most prominent thermal anomaly in the mantle (*8*, *9*). However, global travel-time tomography showed only moderate anomalies of fast *P*- and *S*-wave speeds (V_P and V_S) in the lower mantle along the Tonga subduction zone (*10*, *11*), implying that a large amount of subducted material remains in the upper mantle. If so, how are large-scale remnants of slab accommodated in the transition zone? This issue pertains to the current search for a primordial mantle (*12*, *13*). The more slab material that remains in the transition zone, the easier it is to preserve a primordial component in the lower mantle.

It is a basic tenet of plate tectonics that earthquakes deeper than about 100 km occur in the cold interior of subducted lithosphere (*14–16*). Otherwise, deep earthquakes would not be restricted to zones of recent convergence. Many researchers have noted the complexity of seismicity in the Tonga-Fiji region (*17*, *18*). A unique feature is a subhorizontal swath of deep (>300 km) outboard earthquakes that extends several hundred kilometers farther to the west of the Wadati-Benioff zone (WBZ) (*19*, *20*). The WBZ, which marks the trace of actively subducting lithosphere, is defined by an inclined zone of seismicity connecting shallow earthquakes near the trench with the deepest earthquakes in the mantle (Figs. 1 and 2).

The wide extent of the outboard earthquakes provides a favorable configuration for modeling high-resolution, broadband *P* and *S* waveforms to precisely determine V_P and V_S of the earthquake-generating (seismogenic) material (*21*, *22*). In the transition zone of the mantle, seismic wave speeds are mainly a function of temperature and petrology. In the source region of outboard earthquakes, seismicity independently indicates cold temperature, a condition expected to raise both V_P and V_S. However, a petrologic anomaly to trigger the outboard earthquakes could counteract the thermal effect on wave speeds—a key point to bear in mind.

Here, we first seek to unravel the perplexing pattern of deep seismicity beneath Tonga (Fig. 1). The data include well-determined fault plane solutions of 1000 large- to moderate-sized earthquakes (*17*, *20*, *23–27*) and precise locations of 6600 hypocenters (*28*, *29*). The results are then combined with spatial variations of V_P and V_S to show that a remnant slab lies subhorizontally above the active, steep-dipping WBZ.

To illustrate the relation between the outboard earthquakes and the WBZ, we examine a sequence of 18 cross sections normal to the trench and parallel to the direction of active convergence. For the cross section A–A′ (Figs. 1 and 2A), a continuous band of seismicity, extending from near the surface to depths close to 700 km, defines a clear WBZ with an average dip of about 60°. In addition, fault plane solutions for events in the WBZ show a uniform pattern of down-dip compression, with the axes of maximum com-

[1]Department of Geology, University of Illinois, Urbana, IL 61801, USA. [2]Mid-America Earthquake (MAE) Center, University of Illinois, Urbana, IL 61801, USA.

*To whom correspondence should be addressed. E-mail: w-chen@uiuc.edu

pression (P axes) closely following the dip of slab as revealed by the distribution of seismicity alone. Down-dip compression is a classic pattern for deep earthquakes in all WBZs that reach deep into the transition zone of the mantle, reflecting increasing resistance encountered by the actively subducting lithosphere (*15*, *30*).

A group of outboard earthquakes stands out near the northwestern end of this cross section (point A, Fig. 1), forming a subhorizontal band near a depth of 500 km (Fig. 2A). This cluster of events lies about 200 km above the deepest end of the WBZ, making it difficult to connect the outboard earthquakes with the actively subducting lithosphere. This notion is reinforced by the observation that at a confidence level above 95%, P axes of these outboard earthquakes lie away from the tight grouping of down-dip compression in the WBZ (Fig. 2A). This characteristic in fault plane solutions also holds true for another cluster of events near depths of 300 to 400 km (dashed box, Fig. 2A). In this case, the outboard earthquakes form a dipping band lying about 50 km above the WBZ. At this particular location, there has been no seismicity in the past 35 years to connect the two clusters of outboard earthquakes. Nevertheless, both their fault plane solutions and spatial distributions are distinct from events in the WBZ (Fig. 2A).

Collectively, cross sections throughout the Tonga subduction zone reveal the southern limit of outboard earthquakes to be well defined near 22°S (Fig. 1). Patterns in seismicity and fault plane solutions similar to those depicted in Fig. 2A extend northeastward for over 500 km, close to cross section B–B′ (Fig. 1). At this location, deep seismicity seems to bend sharply northwestward, whereas the WBZ at depths above 300 km retains its approximately planar geometry through the entire subduction zone (Fig. 1). In previous studies, under the assumption that all earthquakes occur in a single, coherent piece of slab, this is where extreme deformation must take place within the slab (*17*, *18*, *31*). In such a scenario, the amount of lateral strain far exceeds 10%, and sharp steps must occur along the dip (*32–34*).

When patterns in fault plane solutions and seismicity of this region are examined simultaneously, it becomes apparent that complex seismicity is a consequence of juxtaposing outboard earthquakes over the WBZ. In cross section B–B′ (Fig. 2B), a clear distinction between outboard earthquakes and those in the WBZ is made by using the same criterion for down-dip compression established in Fig. 2A. Earthquakes below 500 km fall into two groups that are spatially separated and exhibit different fault plane solutions, resembling the observation at depths near 400 km along cross section A–A′ (dashed box, Fig. 2A).

An important constraint on the nature of the outboard earthquakes comes from the seismic properties of the seismogenic region. We recently reported three-dimensional (3D) variations of V_P and V_S and their relation with outboard earthquakes south of Fiji (*21*, *22*). On the basis of a sequence of seismic profiles in a fan-shot geometry, the lateral extent of anomalous V_P and V_S is constrained by comparing results from a wide range of azimuths. This approach uses information from triplicate P and S arrivals that are sensitive to seismic wave speeds at the depths of interest (Fig. 2A). Using additional broadband seismograms recorded at station PVC (Fig. 1), we have now extended the observations to cover the seismogenic zone of nearly all outboard earthquakes south of 15°S (Figs. 1 and 3) (*35*).

Cold temperature, as evident from the widespread distribution of outboard earthquakes, is expected to increase seismic wave speeds (*36*, *37*). However, in the transition zone, prominent anomalies of fast V_P and V_S only occur south of 22°S where no outboard earthquakes are observed. In fact, outboard earthquakes occur in regions where V_P and V_S are ~3% slower than in the region immediately south of 22°S. Evidence for this seem-

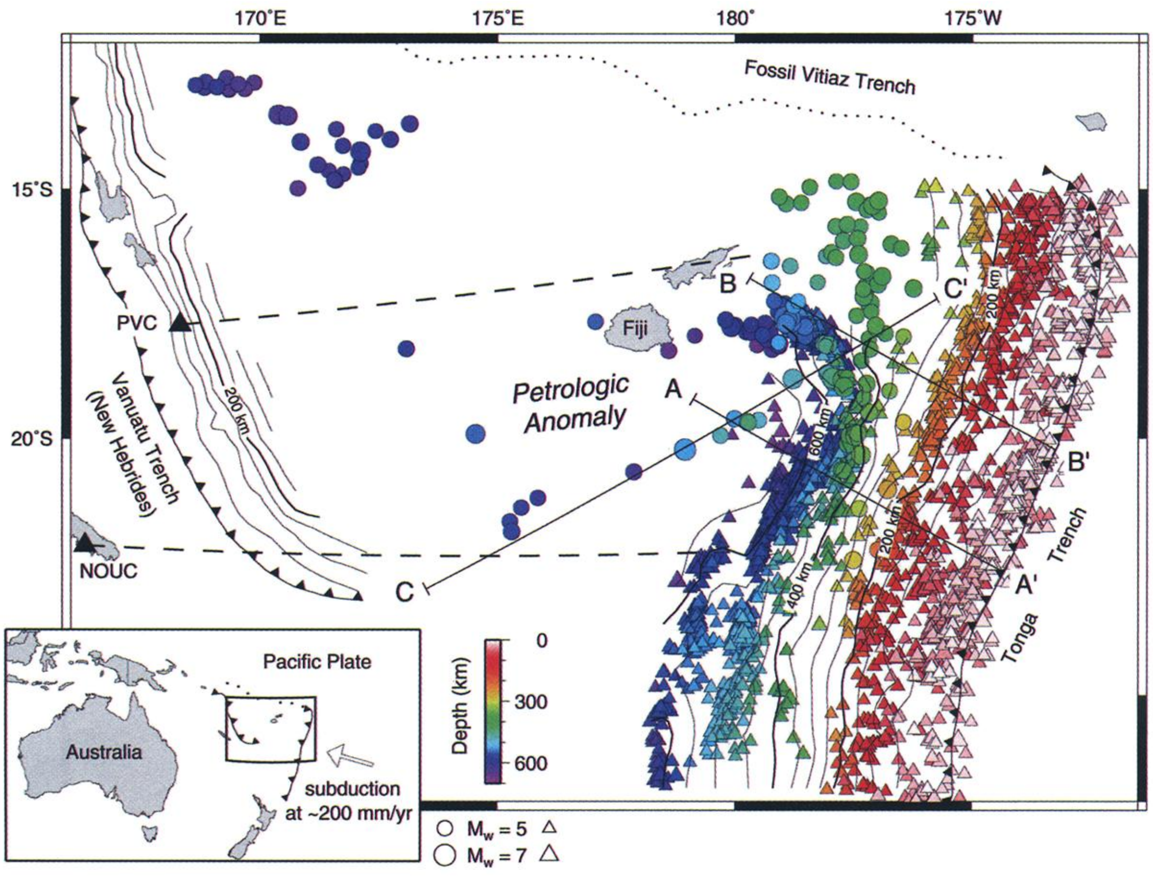

Fig. 1. Map showing hypocenters of large- to moderate-sized earthquakes ($m_b \geq 5$) that occurred between 1964 and 1999 in the TongaFiji region. Contour lines mark depths to the Wadati-Benioff zone (WBZ), defined by earthquakes showing characteristic down-dip compression (triangles). The remaining seismicity is identified as outboard earthquakes (solid circles), extending nearly 1000 km farther west of the WBZ. The dashed lines indicate the lateral extent of a petrologic anomaly that accompanies the outboard earthquakes as identified from lateral variations in V_p and V_s. Solid curves mark the center of key cross sections shown in Fig. 2. To avoid clutter in map view, we show fault plane solutions only in cross sections (Fig. 2). The inset shows the overall tectonic setting of the Tonga subduction zone. PVC and NOUC are broadband seismic observatories whose data are used to determine lateral variations in V_p and V_s.

ingly counterintuitive result is strong. South of 22°S, V_P is fast, such that rays bottoming within the transition zone arrive up to 2 s ahead of shorter rays that bottom just above the transition zone. The opposite is observed in seismogenic zones of outboard earthquakes, resulting in a contrast of up to 4 s in differential travel times for paths flanking 22°S. Thus, the effect of cold temperature in the source region of outboard earthquakes must have been counteracted by a petrologic anomaly, such as compositional or mineralogical variations (*22*).

Two leading candidates for the petrologic anomaly are the presence of metastable olivine (α-phase) or volatiles (*38*). Both will lower seismic wave speeds in the transition zone and could trigger deep earthquakes (*39–47*). Either way, those materials must be brought down to the transition zone by subduction. It follows that outboard earthquakes occur in a region where substantial impounding of subducted material occurs, such that conditions are favorable for the accumulation of metastable olivine or volatiles (*22*).

Overall, the outboard earthquakes have a subhorizontal configuration (Figs. 2C and 3). In a southwest-northeast–trending cross section that excludes events in the WBZ (Fig. 2C), the large- to moderate-size outboard events outline a shallow-dipping, slablike feature. The 3D distribution of outboard earthquakes shows the same configuration over a large region of at least 1000 km by 500 km (Fig. 3), suggesting that the outboard earthquakes occur in a large-scale remnant of subducted lithosphere (*48*).

At the present, it appears that this remnant slab is not attached to actively subducting lithosphere (Fig. 2, A and B). A natural source for the detached lithosphere would be past subduction of the Pacific plate along the

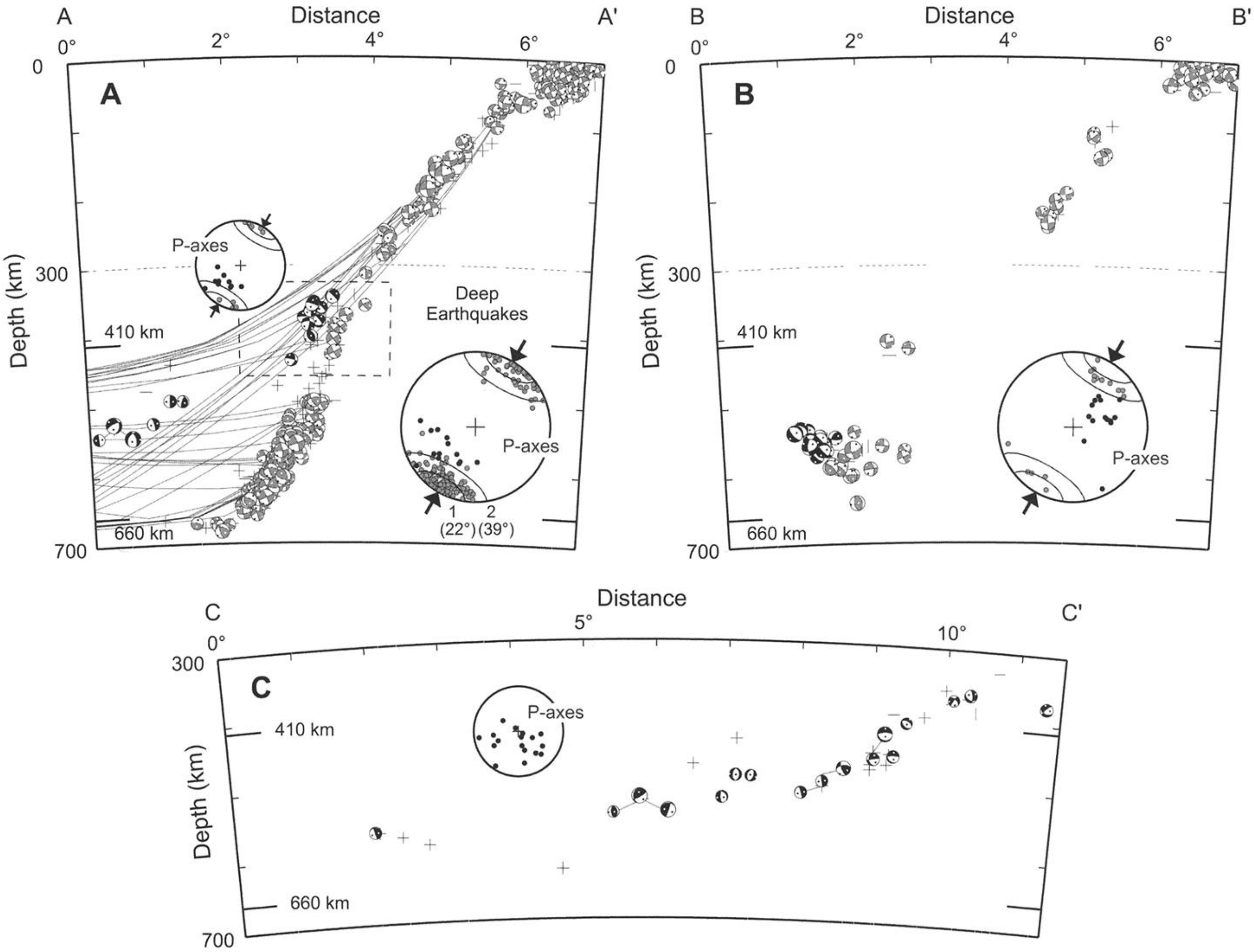

Fig. 2. Three cross sections showing the relation between outboard earthquakes (black shading in fault plane solutions) and events in the active WBZ (gray shading). Fault plane solutions are equal-area projections of the northern hemispheres of the focal spheres, with *P* and *T* axes plotted as solid and open circles, respectively. The size of each fault plane solution is proportional to M_w, with shaded quadrants representing compressional first motions. Crosses show hypocenters with no fault plane solutions available. (**A**) Cross section A–A′. With the same layout as in the fault plane solutions, the large, circular inset shows orientations of *P* axes for all earthquakes deeper than 300 km. For earthquakes in the WBZ (gray circles), notice the tight grouping of *P* axes around the down-dip direction (paired arrows), with a standard deviation of only 22°. All but one of the outboard earthquakes show *P* axes (black circles) that fall at least 2 SDs away from this grouping. This pattern remains for earthquakes enclosed in the dashed box (small, circular inset) where the outboard earthquakes are separated from the WBZ by 50 ± 20 km. Thin, solid curves are representative ray paths used in modeling broadband *P* and *S* waveforms recorded at stations NOUC and PVC—the basis for establishing a petrologic anomaly associated with the outboard earthquakes (Fig. 1). Width of the cross section is 230 km. (**B**) Cross section B–B′, in a region where the trend of deepest seismicity appears to bend sharply to the northwest. With the same criterion as in Fig. 2A, outboard earthquakes are easily distinguished from the WBZ (circular inset). Because of the intense seismicity at depths below 500 km, only events of m_b > 5.5 are plotted over a width of 180 km. (**C**) Cross section C–C′, showing the overall configuration of outboard earthquakes by excluding events in the WBZ. Width of the cross section is 125 km.

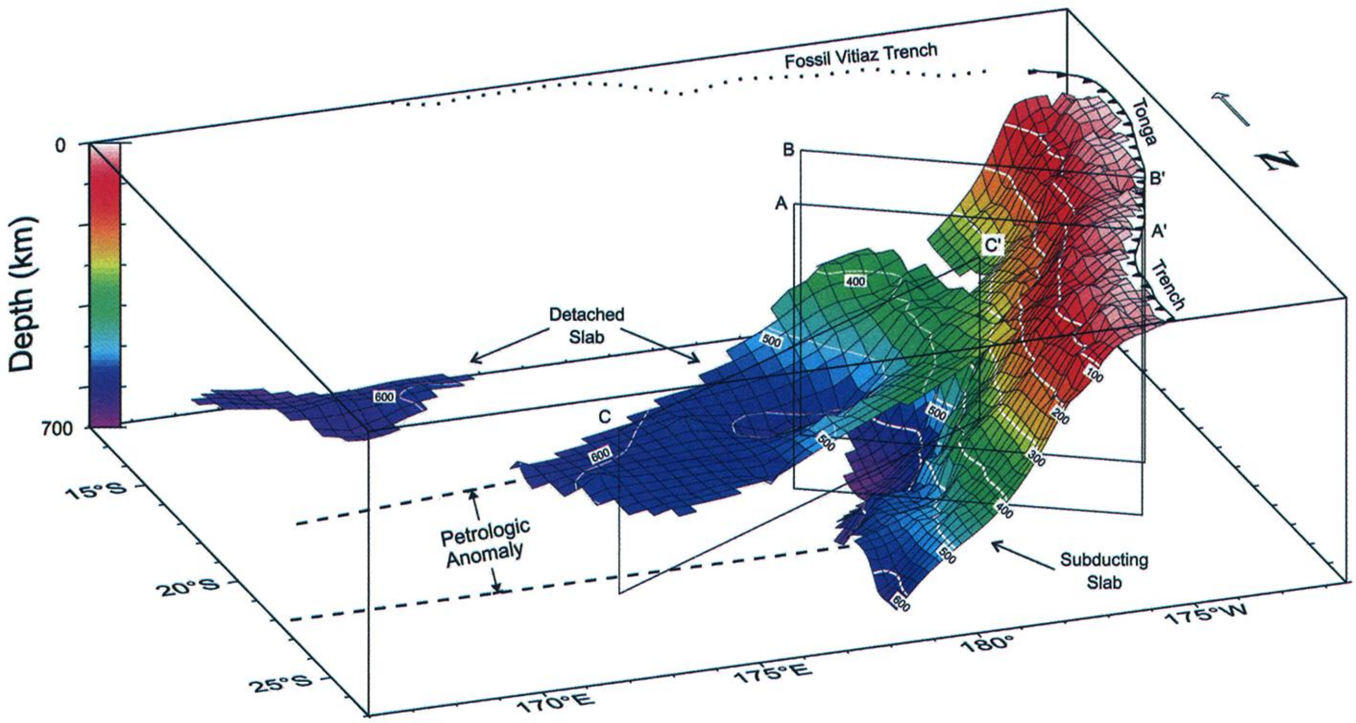

Fig. 3. A 3D rendition of seismicity beneath the Tonga back-arc (with no vertical exaggeration). For the region south of 15°S, two separate surfaces, representing a detached remnant of slab and the actively subducting lithosphere, are constructed from hypocenters of outboard earthquakes and those in the WBZ, respectively. An additional surface indicates the isolated cluster of earthquakes northeast of the Vanuatu trench (*19*, *20*, *48*). Contour lines are drawn at intervals of 100 km in depth. Solid frames indicate cross sections plotted in Fig. 2. The juxtaposition of slabs retains a large amount of subducted material above the lower mantle.

fossil Vitiaz trench where subduction ceased about 5 to 8 million years ago (*17*, *19*, *20*, *32*, *49*). However, it would be very difficult to unravel the detailed history of the detached slab, because it would leave little trace in the geologic record near the surface.

We note that the detached slab is resting subhorizontally in the transition zone of the mantle (Figs. 2C and 3). This configuration may be related to the nature of the petrologic anomaly associated with the remnant slab, because the amount of metastable olivine or hydrous minerals needed to reduce V_P and V_S by 2 to 3% is also expected to make the slab buoyant (*20*, *43*, *50*). It follows that for metastable olivine, the buoyancy of the slab is a self-limiting process of floating and sinking confined to the transition zone (*22*, *51*). Such a scenario would explain why outboard earthquakes occupy such a thick region over the entire depth range of the transition zone (Fig. 2C).

In any case, all the evidence suggests that outboard earthquakes are manifestations of a remnant slab that lies subhorizontally above the active, steep-dipping WBZ. This configuration is distinct from that of previous proposals to retain subducted lithosphere in the upper mantle, such as impounding of material upon the 660-km discontinuity ("megalith") (*52*) or subhorizontal extension of the WBZ (*53*–*55*). The juxtaposition of a large-scale subhorizontal slab remnant and a steep-dipping WBZ retains a large amount of subducted material in the upper mantle. In cross-sectional view, the overall length of slab in the upper mantle exceeds 2000 km (Fig. 2A). This conclusion provides a natural explanation for the lack of a prominent slab signature in the lower mantle along the Tonga subduction zone.

Isotopic signatures of ocean island basalts have long pointed to a primordial component of the lower mantle that remains isolated from the mixing caused by plate tectonic cycles (*56*–*58*). The exact location and nature of this component are a matter of ongoing research with contradictory results (*13*, *59*). If the configuration of remnant slabs shown in Fig. 3 has occurred elsewhere in the past, a substantial amount of slab material may not readily enter the lower mantle, allowing considerable leeway to preserve a primordial component in the lower mantle (*60*).

References and Notes

1. T. Lay, *Annu. Rev. Earth Planet. Sci.* **22**, 33 (1994).
2. P. G. Silver, R. W. Carlson, P. Olson, *Annu. Rev. Earth Planet. Sci.* **16**, 477 (1988).
3. The top of the lower mantle is marked by a major seismic discontinuity near the depth of 660 km. Between depths of 410 and 660 km is the transition zone of the mantle, which is sometimes defined as part of the upper mantle.
4. C. G. Chase, *Geol. Soc. Am. Bull.* **82**, 3087 (1971).
5. C. Lithgow-Bertelloni, M. Richards, *Rev. Geophys.* **36**, 27 (1998).
6. M. A. Richards, D. C. Engebretson, *Nature* **355**, 437 (1992).
7. M. Bevis *et al.*, *Nature* **374**, 249 (1995).
8. D. P. McKenzie, *Tectonophysics* **10**, 357 (1970).
9. S. Stein, C. A. Stein, in *Subduction Top to Bottom*, G. E. Bebout *et al.*, Eds. (American Geophysical Union, Washington, DC, 1996), vol. 96, pp. 1–17.
10. S. P. Grand, R. D. van der Hilst, S. Widiyantoro, *GSA Today* **7**, 1 (1997).
11. R. D. van der Hilst, S. Widiyantoro, E. R. Engdahl, *Nature* **386**, 578 (1997).
12. F. Albarède, R. D. van der Hilst, *Eos* **80**, 535 (1999).
13. J. E. Vidale, G. Schubert, P. S. Earle, *Geophys. Res. Lett.* **28**, 859 (2001).
14. B. Isacks, J. Oliver, L. R. Sykes, *J. Geophys. Res.* **73**, 5855 (1968).
15. B. Isacks, P. Molnar, *Rev. Geophys.* **9**, 103 (1971).
16. P. Molnar, D. Freedman, J. S. F. Shih, *Geophys. J. R. Astron. Soc.* **56**, 41 (1979).
17. S. Billington, thesis, Cornell University, Ithaca, NY (1980).
18. D. Giardini, J. H. Woodhouse, *Nature* **307**, 505 (1984).
19. M. W. Hamburger, B. L. Isacks, *J. Geophys. Res.* **92**, 13841 (1987).
20. E. A. Okal, S. H. Kirby, *Phys. Earth Planet. Inter.* **109**, 25 (1998).
21. M. R. Brudzinski, W.-P. Chen, *Eos* **80**, F667 (1999).
22. ———, *J. Geophys. Res.* **105**, 21661 (2000).
23. A. M. Dziewonski, T.-A. Chou, J. H. Woodhouse, *J. Geophys. Res.* **86**, 2825 (1981).
24. F. M. Richter, *J. Geophys. Res.* **84**, 6783 (1979).
25. F. N. Skomurski, M. R. Brudzinski, W.-P. Chen, *Eos* **80**, F667 (1999).
26. D. A. Wiens, J. J. McGuire, P. J. Shore, *Nature* **364**, 790 (1993).
27. When more than one solution was available for a given event, we used the solution obtained by detailed waveform inversion.

28. E. R. Engdahl, R. D. van der Hilst, R. P. Buland, *Bull. Seismol. Soc. Am.* **88**, 722 (1998).
29. Epicenters are those relocated by Engdahl *et al.* (*28*) and their latest updates. We compared this data set with detailed relocation of a dozen events in the Tonga-Fiji region by Wiens *et al.* (*26*). The difference in epicenters is less than 5 km in most cases and never exceeds 10 km. When available, we used precise focal depths of over 200 events determined by Brudzinski and Chen (*21, 22*) who modeled the time interval between phases *pP* and *P* using a seismic velocity model specifically developed for this region. On average, focal depths reported by Engdahl *et al.* (*28*) are off by only ±8 km. Thus, the data set used in this study is sufficient to resolve if earthquakes are associated with the active WBZ.
30. B. Isacks, P. Molnar, *Nature* **233**, 1121 (1969).
31. D. Giardini, J. H. Woodhouse, *Nature* **319**, 551 (1986).
32. K. Fischer, K. C. Creager, T. H. Jordan, *J. Geophys. Res.* **96**, 14403 (1991).
33. K. S. Strobach, *Z. Geophys.* **39**, 819 (1973).
34. K. Yamaoka, Y. Fukao, M. Kumazawa, *Rev. Geophys.* **24**, 27 (1986).
35. For this study, we analyzed 50 additional triplicate *P* and *SH* waveforms to extend northward the coverage offered by 270 waveforms in Brudzinski and Chen (*21, 22*).
36. K. C. Creager, T. H. Jordan, *J. Geophys. Res.* **91**, 3573 (1986).
37. S. Kern, Ed., *P- and S-Wave Velocities in Crustal and Mantle Rocks Under the Simultaneous Action of High Confining Pressure and High Temperature and the Effect of the Rock Microstructure* (Schweizerbart, Stuttgart, Germany, 1982).
38. The latter could be either hydrous minerals or free fluids, such as water or even partial melt (*21, 22*).
39. U. H. Faul, D. R. Toomey, H. S. Waff, *Geophys. Res. Lett.* **21**, 29 (1994).
40. H. Fujisawa, *J. Geophys. Res.* **103**, 9591 (1998).
41. H. W. Green, P. C. Burnley, *Nature* **341**, 733 (1989).
42. H. W. Green, H. Houston, *Annu. Rev. Earth Planet. Sci.* **23**, 169 (1995).
43. T. Inoue, D. J. Weidner, P. A. Northrup, J. B. Parise, *Earth Planet. Sci. Lett.* **160**, 107 (1998).
44. T. Katsura, E. Ito, *J. Geophys. Res.* **94**, 15663 (1989).
45. S. H. Kirby, W. B. Durham, L. A. Stern, *Science* **252**, 216 (1991).
46. C. Meade, R. Jeanloz, *Science* **252**, 68 (1991).
47. P. G. Silver *et al.*, *Science* **268**, 69 (1995).
48. The configuration of the slab remnant shown in Fig. 3 includes the group of isolated deep earthquakes near 15°S and 170°E. Despite a large aseismic region between 15° and 18°S, the distribution of hypocenters and fault plane solutions of the isolated earthquakes is similar to those illustrated in Fig. 2C (*19, 20, 61*). At the present, however, it is unknown if a petrologic anomaly accompanies this cluster of earthquakes, or if this cluster is attached to other outboard earthquakes.
49. M. Barazangi, B. L. Isacks, J. Oliver, J. Dubois, G. Pascal, *Nature* **242**, 98 (1973).
50. C. R. Bina, *Geophys. Res. Lett.* **23**, 3563 (1996).
51. Only the portion of slab below the 410-km discontinuity becomes buoyant because of metastable α-phase (50, 62). However, this portion will never float above the 410-km discontinuity where warmer olivine of the ambient mantle is also in α-phase.
52. A. E. Ringwood, T. Irifune, *Nature* **331**, 131 (1988).
53. Y. Fukao, M. Obayashi, H. Inoue, M. Nenbai, *J. Geophys. Res.* **97**, 4809 (1992).
54. P. M. Shearer, T. G. Masters, *Nature* **355**, 791 (1992).
55. R. D. van der Hilst, E. R. Engdahl, W. Spakman, *Geophys. J. Int.* **115**, 264 (1993).
56. C. Y. Chen, F. A. Frey, *Nature* **302**, 785 (1983).
57. L. H. Kellogg, B. H. Hager, R. D. van der Hilst, *Science* **283**, 1881 (1999).
58. D. L. Turcotte, D. Paul, W. M. White, *J. Geophys. Res.* **106**, 4265 (2001).
59. R. D. van der Hilst, H. Kárason, *Science* **283**, 1885 (1999).
60. Slab material would be difficult to detect with routine seismological experiments when thermal and petrologic effects on seismic wave speeds counteract each other.
61. S. H. Kirby, S. Stein, E. A. Okal, D. C. Rubie, *Rev. Geophys.* **34**, 261 (1996).
62. F. C. Marton, C. R. Blina, S. Stein, D. C. Rubie, *Geophys. Res. Lett.* **26**, 119 (1999).
63. H. Green and an anonymous reviewer provided helpful reviews. Supported by the NSF.

17 January 2001; accepted 21 May 2001

A Mite Species That Consists Entirely of Haploid Females

Andrew R. Weeks,[1]* Frantisek Marec,[2] Johannes A. J. Breeuwer[1]

The dominance of the diploid state in higher organisms, with haploidy generally confined to the gametic phase, has led to the perception that diploidy is favored by selection. This view is highlighted by the fact that no known female organism within the Metazoa exists exclusively (or even for a prolonged period) in a haploid state. We used fluorescence microscopy and variation at nine microsatellite loci to show that the false spider mite, *Brevipalpus phoenicis*, consists of haploid female parthenogens. We show that this reproductive anomaly is caused by infection by an undescribed endosymbiotic bacterium, which results in feminization of haploid genetic males.

It is commonly thought that no female organism within the Metazoa exists exclusively in a haploid state, because selection favors diploidy in higher organisms (*1*, *2*). There are several theories about the evolution of diploidy as the dominant state, and deleterious mutations (germline and/or somatic) are considered to be the driving force (*3*, *4*). Yet experimental evidence is lacking, and currently no studies on life cycle evolution have been conducted in a higher organism.

Brevipalpus phoenicis Geijskes (Acari: Tenuipalpidae) is a minute phytophagous mite found throughout tropical and subtropical regions. It is polyphagous and is a major pest of many economically important crops such as citrus, coffee, tea, papaya, passion fruit, and palms (*5*). In citrus, it acts as a vector for citrus leprosis virus (Rhabdoviridae), a disease that causes millions of dollars of damage to the Brazilian citrus industry each year (*6*). *Brevipalpus phoenicis*, along with two closely related species, *B. obovatus* and *B. californicus*, is known to reproduce by thelytokous (obligate) parthenogenesis (*7*). Rare males are found in field populations; however, their function is not known (*8*). The closest sexual relative, *B. russulus*, is haplodiploid, in which unfertilized eggs develop into haploid males (two chromosomes) whereas fertilized eggs develop into diploid females (four chromosomes) (*9*). Haplo-diploidy is characteristic of their superfamily, the Tetranychoidea. All three parthenogenetic species have only two chromosomes in somatic cells (Fig. 1A) (*10*); however, owing to the small size of these chromosomes and their apparent lack of any distinguishable morphological character, it is not known whether this represents the haploid or diploid state.

Although it has been proposed that *B. obovatus* is a haploid parthenogen (*7*, *9*), convincing cytological evidence has been lacking (*11*, *12*). Cytological techniques using fluorescence microscopy provide an accurate way to determine whether these three species are haploid or diploid parthenogens. We used two such techniques, as well as genetic variation at nine microsatellite loci, to show that *B. phoenicis* is indeed a haploid female parthenogen.

Brevipalpus phoenicis females collected from a coffee plantation at the University of Sao Paulo, Piracicaba, Sao Paulo, Brazil, were used to initiate five isofemale lines (lines started with a single immature female) from which eggs were used for the following experiments. Using a fluorescent dye (YOYO-1, Molecular Probes) that stains both DNA and RNA, we visualized the nuclear organizing region (NOR), which is present during early prophase in mitotic divisions in eggs of *B. phoenicis* (*13*, *14*). Homologous pairs of chromosomes will have a NOR or NORs at exactly the same position. We found one NOR to be present during early prophase mitotic divisions in 2-day-old eggs (Fig. 1, B and C) from *B. phoenicis*. The NOR was found at the tip of one chromosome, with no corresponding NOR being present on the second chromosome.

To complement the finding of a single NOR, we also used fluorescent in situ hybridization (FISH) to locate the ribosomal DNA

[1]Institute for Biodiversity and Ecosystem Dynamics, Sections Population Biology and Evolutionary Biology, University of Amsterdam, 1098 SM Amsterdam, Netherlands. [2]Institute of Entomology, Czech Academy of Sciences, CZ-370 05 Ceske Budejovice, Czech Republic.

*To whom correspondence should be addressed at the Centre for Environmental Stress and Adaptation Research, Department of Biological Sciences, Monash University, Clayton 3168, Australia. E-mail: Andrew.Weeks@sci.monash.edu.au